ELSEVIER

Contents lists available at ScienceDirect

### Science of the Total Environment

journal homepage: www.elsevier.com/locate/scitotenv



# Efficient adsorptive removal of short-chain perfluoroalkyl acids using reed straw-derived biochar (RESCA)



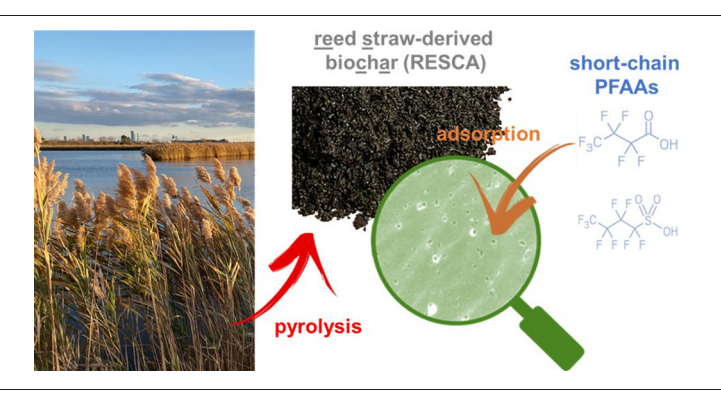
Na Liu <sup>a,b</sup>, Chen Wu <sup>a</sup>, Guifen Lyu <sup>a,c</sup>, Mengyan Li <sup>a,\*</sup>

- a Department of Chemistry and Environmental Science, New Jersey Institute of Technology, Newark, NJ 07102, United States
- <sup>b</sup> School of Earth Sciences and Resources, China University of Geosciences, Beijing 100083, China
- <sup>c</sup> Key Laboratory of Jiangxi Province for Persistent Pollutants Control and Resources Recycle, Nanchang Hangkong University, Nanchang 330063, China

#### HIGHLIGHTS

- Reed straw-derived biochar (RESCA) showed effective removal of shortchain PFAAs.
- Surface hydrophobicity and uniform mesopores contribute to its fast adsorption kinetics.
- Presence of high DOC (e.g., >8 mg/L) in groundwater hinders PFAA adsorption.
- Sequential GAC and RESCA adsorption is recommended for the cleanup of mixed

#### GRAPHICAL ABSTRACT



#### ARTICLE INFO

Article history: Received 10 June 2021 Received in revised form 14 July 2021 Accepted 18 July 2021 Available online 20 July 2021

Editor: Deyi Hou

Reywords:
Per- and polyfluoroalkyl substances (PFAS)
Perfluoroalkyl acids (PFAA)
Adsorption
Granular activated carbon (GAC)
Biochar
Perfluorooctanoic acid (PFOA)
Perfluorooctanesulfonic acid (PFOS)
Perfluorobutanoic acid (PFBA)

#### ABSTRACT

Drinking water and groundwater treatment of perfluoroalkyl acids (PFAAs) heavily relies on adsorption-based approaches using carbonaceous materials, such as granular activated carbon (GAC). Application of GAC is restricted by its inefficiency to remove short-chain PFAAs that have prevalently emerged as substitutes and/or metabolites of long-chain polyfluoroalkyl and perfluoroalkyl substances (PFAS). Here, we synthesized reed strawderived biochar (RESCA) exhibiting exceptional removal efficiencies (>92%) toward short-chain PFAAs at environment-relevant concentrations (e.g., 1 µg/L). Pseudo-second-order kinetic constants of RESCA were 1.13 and 1.23 L/(mg h) for perfluorobutanoic acid (PFBA) and perfluorobutanesulfonic acid (PFBS), respectively, over six times greater than GAC. SEM imaging and BET analysis revealed the combination of highly hydrophobic surface and scattered distribution of mesopores (2–10 nm in diameter) was associated with the rapid adsorption of short-chain PFAAs. RESCA-packed filters demonstrated effective removal of the mixture of three short-chain and three long-chain PFAAs in the influent with the flow rate up to 45 mL/min. In contrast, GAC-packed filters were significantly less efficient in the removal of short-chain PFAAs, which were also negatively affected by the increase of the flow rate. Efficacy of RESCA-packed filters was also validated in four PFAA-spiked groundwater samples from different sites. Dissolved organic matter (DOC) of >8 mg/L can negatively affect the removal of short-chain PFAAs by RESCA. Feasibility of scaling up the RESCA adsorption system was investigated using breakthrough simulation. Overall, RESCA represents a green adsorbent alternative for the feasible and scalable treatment of a wide spectrum of PFAAs of different chain lengths and functional moieties.

© 2021 Elsevier B.V. All rights reserved.

\* Corresponding author. E-mail address: mengyan.li@njit.edu (M. Li).

#### 1. Introduction

Perfluoroalkyl acids (PFAAs) have emerged with rising concerns given their prevalent detection worldwide in water, sediment, soil, air, and biota (Jahnke et al., 2009; Kim and Kannan, 2007; Paul et al., 2008). PFAAs are extremely persistent and can spread through the passage of the food web, posing imminent threats to human health and ecosystems (Buck et al., 2011; Giesy and Kannan, 2001; Harris et al., 2017; Nartey and Zhao, 2014; Poothong et al., 2020). Primary attention has been long centered on long-chain PFAAs ( $C \ge 6$  for sulfonic acids and  $C \ge 8$  for carboxylic acids), particularly perfluorooctanoic acid (PFOA) and perfluorooctanesulfonic acid (PFOS), which are lipophilic conferring high bioaccumulation potentials (Table S1). Accordingly, EPA has established a stringent health advisory level of 70 ng/L for the combination of PFOA and PFOS, corresponding to a  $10^{-6}$  lifetime cancer risk (USEPA, 2016).

Current treatment of PFAA-impacted water extensively relies on adsorption-based approaches (Kucharzyk et al., 2017; Ross et al., 2018). Granular activated carbon (GAC) and resin are effective in removing PFOS, PFOA, and many other long-chain PFAAs that have been primarily targeted by regulatory agencies and responsible parties (Deng et al., 2010; Guo et al., 2017; Ross et al., 2018; Xiao et al., 2017). However, field application of GAC and resin is restricted by their limited efficiency to remove short-chain PFAAs, such as perfluorobutanoic acid (PFBA), perfluorobutanesulfonic acid (PFBS), and perfluorohexanoic acid (PFHxA), due to their reduced hydrophobicity (Du et al., 2015; McCleaf et al., 2017a). With the advancement in the coverage and sensitivity of PFAS analytical approaches, short-chain PFAAs have been reported at growing frequencies at aqueous film forming foams (AFFFs)impacted sites and diverse environmental compartments (Andersson et al., 2019; Brendel et al., 2018; Dauchy et al., 2019; Guelfo and Higgins, 2013; Higgins et al., 2017; Lang et al., 2017; Li et al., 2020; Liu et al., 2019). Prevalence of short-chain PFAAs is attributed to the increase of manufacture, use, and discharge of short-chain PFAAs and related precursor compounds (typically polyfluorinated with nonfluorinated moieties) in the past decade since the phase-out of longchain PFAAs (Brendel et al., 2018). Short-chain PFAAs are highly soluble and mobile, conducive to dilute contamination in a greater region distant from the source. Short-chain PFAAs also tend to enrich in edible parts (e.g., fruits and leaves) of plants, incurring human exposure risks (Blaine et al., 2013; Felizeter et al., 2012). Though relatively less bioaccumulable, short-chain PFAAs can bind serum albumin and other proteins, which concentrate in blood-rich organs (Bischel et al., 2011; Bogdanska et al., 2014; Burkemper et al., 2017). Collectively, the combination of persistence, prevalence, and toxicity of short-chain PFAAs underscores the need to develop effective and economical technologies applicable for water treatment and remediation.

Biochar is a green alternative for GAC and other fabricated carbonaceous adsorbents, since it is made from biowastes via pyrolysis, a thermal decomposition process in absence of oxygen (Lehmann and Joseph, 2009). Recent studies have assessed PFAA adsorption removal using biochars that were derived from pine needle (Xiao et al., 2017), wood (Dalahmeh et al., 2019; Inyang and Dickenson, 2017; Kupryianchyk et al., 2016; Zhang et al., 2019), corn straw (Guo et al., 2017), or paper mill waste (Kupryianchyk et al., 2016). However, these biochars didn't exhibit superior kinetics or capacities in PFAA adsorption compared to the commercial adsorbent GAC. As shown in Table S2, previous biochars either exhibited uneven removal efficiencies in the ranges of 30% ~ 94% and 15% ~ 87% for the long-chain and shortchain PFAAs, respectively. These biochars also showed either low adsorption capacity (e.g., 0.002 mg/g) and/or prolonged equilibrium (e.g., >3 days), precluding them from field applications (Inyang and Dickenson, 2017).

We noted that the adsorption performance of biochar is governed by the choice of feedstock materials and pyrolysis conditions (e.g., temperature and duration) (Agrafioti et al., 2013). Different feedstocks are varied in chemical components (e.g., cellulose, hemicellulose, and lignin) and physical structures and can form biochars of diverse properties (e.g., pore size and distribution, surface and internal chemistry, and hydrophobicity) through carbonization under varying pyrolysis conditions. In this study, we synthesized a collection of biochars from different feedstocks at an array of pyrolysis temperatures and durations and evaluated their adsorption toward six PFAAs in comparison with a commercial GAC, Calgon Filtrasorb 820, which has been widely used for the removal of emerging pollutants in water. Six PFAAs (Table S1) included C4, C6, and C8 perfluoroalkyl carboxylates (PFCAs) and sulfonates (PFSAs), representing PFAAs of different chain lengths and functional groups. Surface properties of biochars were characterized to investigate dominant adsorption mechanisms. Mini-filter tests were employed to demonstrate the change of removal efficiencies in response to filtration flow rates and the presence of co-existing dissolved organic carbons (DOCs) in field groundwater. To mimic the scaled-up field application, breakthrough curves were simulated based on the kinetic and isotherm characteristics obtained from the batch assays. This discovery of new biochar adsorbents enabled more efficient and feasible mitigation of short-chain PFAAs, which have been increasingly detected in the field with or without the co-existence of longchain PFAAs and other co-contaminants.

#### 2. Materials and methods

#### 2.1. Feedstock material preparation

Common reeds (*Phragmites australis*) were collected in the dry season (fall and winter) at the Meadowlands (Lyndhurst, NJ). After the removal of leaves and ears, reed straws were cut into pieces of 1–2 cm in length, dried at 100–110 °C in the oven overnight. Corn cobs and soybeans were purchased from a local grocery store in New Jersey. After removal of the seeds, cobs were chopped into small cubes and dried aforementioned. Aspen chips were purchased from a PetSmart™ store. After pureed using a blender, soybean dregs were filtered with cloth and fully dried in the oven at 100–110 °C. All the feedstocks were then kept in a glass vacuum desiccator for further use.

#### 2.2. Biochar synthesis

Approximately 20 g of feedstock materials were transferred to a ceramic holder and placed in an electric dual-zone split tube furnace (OTF-1200, MTI Co., Richmond, CA). Nitrogen was provided from the compressed cylinder to create an inert environment for pyrolysis and purge the exhaust from the chamber. Temperature was increased to the highest temperature (e.g., 500, 700, and 900 °C) at a heating rate of 5 °C/min. Pyrolysis was held at the highest pyrolysis temperature for a duration of 3, 5, or 6 h, before being cooled to room temperature under nitrogen flow. Biochar particles were pulverized and sieved to a particle size of 0.08–0.2 mm, and over 80% of biochar particles (~80%) were in the range of 0.1–0.2 mm.

#### 2.3. Biochar characterization

Surface area and pore size distribution of biochars and GAC were measured with an Automated Gas Sorption Analyzer (Autosorb iQ-MP, Quantachrome Instruments, Boynton Beach, FL) on the basis of nitrogen adsorption isotherms at pressures decreasing from 1 to  $10^{-6}$  atm at 77 K. Surface area was calculated from the monolayer amount using the Brunauere Emmette Teller (BET) method, and pore size distribution was computed based on the Density Functional Theory (DFT) using the graphite model with slit shape geometry (Park et al., 2020).

Surface morphology was examined using a variable pressure scanning electron microscope (JSM-7900F, JEOL, Japan). Fourier-transform infrared spectroscopy (FTIR) was employed to uncover the surface chemistry of the synthesized biochar particles and analyze functional

moieties formed among C, N, O, and H. FTIR spectra of biochar and GAC samples were obtained with a Cary 670 FTIR spectrometer (Agilent, Santa Clara, CA) using the diffuse reflectance accessory at room temperature ( $24 \pm 2$  °C). Spectra were measured from 4000 to 400 cm<sup>-1</sup> at a resolution of 4 cm<sup>-1</sup> and a total of 128 scans were averaged to produce the final spectrum. Assignment of vibrational modes was based on the spectrum table from Badertscher et al. (2009) (Badertscher et al., 2009).

The anion exchange capacity (AEC) of biochars was determined following the method described in Lawrinenko and Laird (2015) (Lawrinenko and Laird, 2015) using bromide as an index anion. Dialyzed biochar (1 g) was suspended in 2 mL of 1 M KBr shaken for two days, and then rinsed with DI water on the 0.45- $\mu$ m PES filter paper until the conductivity of the rinsate was below 5  $\mu$ S cm $^{-1}$ . Biochars were transferred into polypropylene bottles and added with 2 mL of 2.5 M CaCl $_2$  and 50 mL DI water. After being shaken for two days, biochars were filtered through 0.45- $\mu$ m PES filter membrane and the bromide in filtrates was analyzed using a Thermo Scientific Orion Bromide Electrodes (Thermo, Waltham, MA).

#### 2.4. Batch adsorption experiments

Effectiveness of PFAA adsorption was evaluated in batch tests prepared in 30-mL glass flasks containing 2 mg of selected adsorbents (biochar, GAC, and resin) and 10 mL Milli-Q water spiked with individual PFAA at an initial concentration of 1 or 100 µg/L, representing the trace and high PFAA contamination levels in the environment. Flasks were sealed and agitated at 200 rpm on an orbital shaker at room temperature (24  $\pm$  2 °C) for 24 h when the PFAA adsorption reached equilibrium. Then, suspensions were filtered through 0.22 µm PES membrane filters and stored in vials at 4 °C prior to the LC/MS/MS analysis. All experiments were conducted in triplicate and controls were prepared without the addition of adsorbents and corrected for bottle losses. GAC (Calgon Filtrasorb 820) was provided by the Passaic Valley Water Commission (Clifton, NJ) and was sieved to a particle size of 0.1-0.6 mm, which were dominantly in the range of 0.1-0.2 mm (91%). Anion exchange resin (polyethyleneimine on silica beads, 0.4-0.8 mm) was purchased from Alfa Aesar (Haverhill, MA).

For adsorption isotherms, batch experiments were prepared in a similar fashion as described above but initially spiked at PFAA concentrations ranging from 100 to 250,000  $\mu$ g/*L. maximum* sorption capability ( $Q_m$ ) and other parameters were computed by fitting with classic isotherm models (Langmuir and Freundlich) below (Wei et al., 2015).

Langmuir model:

$$Q_e = \frac{Q_m C_e}{K_d + C_e} \tag{1}$$

Freundlich model:

$$Q_e = K_F C_e^{1/n} \tag{2}$$

where  $Q_e$  (mg/g) and  $C_e$  (mg/L) are the amounts of adsorbed PFAA per unit mass of adsorbent and PFAA concentration at equilibrium, respectively;  $Q_m$  (mg/g) is the maximum amount of PFAA per unit mass of adsorbent to form a complete monolayer on the surface;  $K_d$  (mg/L) is a constant related to the affinity of the binding sites on the adsorbent;  $K_F$  and 1/n were the Freundlich model constants, indicating capacity and intensity of adsorption, respectively.

For adsorption kinetics, batch experiments were prepared in 100-mL glass flasks containing 50 mL Milli-Q water spiked with individual PFAA at an initial concentration of 100  $\mu$ g/L. At the beginning and select intervals (up to 5 d), 200  $\mu$ L of supernatant was removed by syringe and filtered for analysis. Kinetics data were fitted using the pseudo-second-order kinetic model below (Blanchard et al., 1984).

Pseudo-second-order kinetic model:

$$\frac{1}{C} - \frac{1}{C_0} = k_2 t \tag{3}$$

where C (mg/L) and  $C_0$  (mg/L) are the PFAA concentrations at different time and initial concentration, respectively;  $k_2$  is the second-order adsorption rate.

To assess the competitive inhibitory efforts between long-chain and short-chain PFAAs, bisolute systems were prepared in batch with the initial concentration of PFBA and PFOA of 100  $\mu$ g/L and the adsorbent/solution ratio of 0.2 g/L. Other conditions were identical with single solute kinetic adsorption experiments described above.

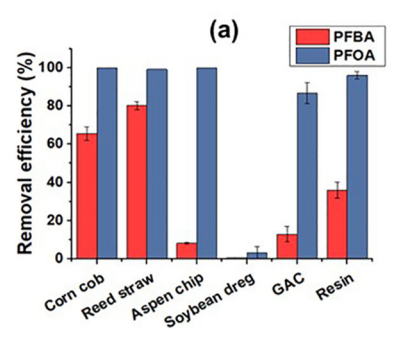
#### 2.5. Mini-filter filtration tests

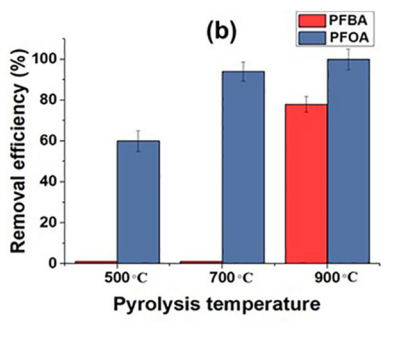
Biochar or GAC (0.1 g) was packed in 12-mL polypropylene columns (1 cm in diameter) with 0.02 g glass wool to plug the outlets. Packed columns were used to filter 10 mL Milli-Q water spiked with a mixture of all six PFAAs (50  $\mu$ g/L each). Flow rates were controlled at 15, 30, and 45 mL/min by using SPE Vacuum Manifold (Thermo, Waltham, MA). Infiltrates were collected and filtered for further analysis. Control columns packed with glass wool only were used to discern the PFAA removal by non-adsorbent compartments of the mini-filters.

To further assess the effectiveness of PFAA removal in environmental samples, four groundwater samples were collected from two sites located in California and New Jersey, US. These groundwater samples contain a wide variety of contaminants (Table S6), such as trichloroethylene, benzene, and 1,4-dioxane, which may co-exist with PFAAs in the field. Each sample (10 mL) was spiked with a mixture of all six PFAAs (50 µg/L each) and filtered through the biochar or GAC-packed minifilters at the flow rate of 30 mL/min. Before and after the filtration, dissolved organic carbon (DOC) of the groundwater samples was measured using a Shimadzu total organic carbon (TOC) analyzer (Japan). Samples were filtered using 0.45 µm membrane filters (MS® mixed cellulose ester, MCE) and acidified with hydrochloric acid (37%, ACS grade, Sigma-Aldrich) to pH 2–3.

#### 2.6. Analysis of PFAAs by LC/MS/MS

PFAA concentrations were analyzed using a 1290 Infinity II HPLC system in tandem with 6470A triple quadrupoles mass spectrometer (LC/MS/MS, Agilent, Santa Clara, CA). Aliquots (1 µL) were injected into the LC/MS/MS system equipped with a Symmetry C18 column (I.D. 2.1 mm, length 100 mm, particle size 3.5 µm) (Waters, Milford, MI) at a flow rate of 0.5 mL/min. The mobile phase initially consisted of 80% solvent A (5 mM ammonia acetate in 10% methanol) and 20% solvent B (pure methanol) and was held for 0.5 min. The subsequent gradient of the mobile phase was programmed as follows: concentration of solvent B was ramped to 30% in 1.5 min, increased gradually to 95% in 6 min, then increased to 100% in 2 min, and then reduced to 20% in 1 min, and held for additional 2 min at the end. Triple quadrupoles mass spectrometer was operated in the negative-ion electrospray mode. Quantitative analysis was performed using selected reaction ion monitoring (SRM). The precursor→product ion values were set for PFBA (213→169), PFBS (299→80), PFHxA (313→269), PFHxS (399→80), PFOA (413→368), PFOS (499→80), respectively. Calibration standards of the mixed PFAS were purchased from Wellington Laboratories. Spiking solutions for all experiments were prepared from standards of perfluoroalkyl carboxylic acids (PFCAs) and perfluoroalkyl sulfonic acids (PFSAs) purchased from Sigma-Aldrich Calibration curves were prepared with mix PFAS standard to achieve a series of concentrations ranging from 0.1 to 100 µg/L. The method detection limits (MDLs) were estimated as PFBA (80 ng/L), PFBS (40 ng/L), PFHxA (80 ng/L), PFHxS (50 ng/L), PFOA (30 ng/L), PFOS (60 ng/L), respectively.





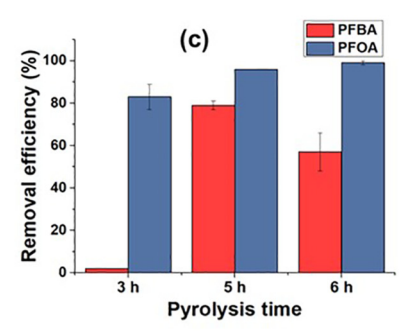


Fig. 1. (a) PFBA and PFOA removal efficiencies exhibited by biochars synthesized with different feedstock materials in comparison with GAC and anion exchange resin; (b) PFBA and PFOA removal efficiencies exhibited by RESCAs synthesized at different pyrolysis temperatures; (c) PFBA and PFOA removal efficiencies exhibited by RESCAs pyrolized at 900 °C for different durations. Removal efficiency was discerned based on the disappearance of the target PFAA after adsorption over 24 h with an initial concentration of 100 μg/L and an adsorbent dose of 0.2 g/L.

#### 3. Results and discussion

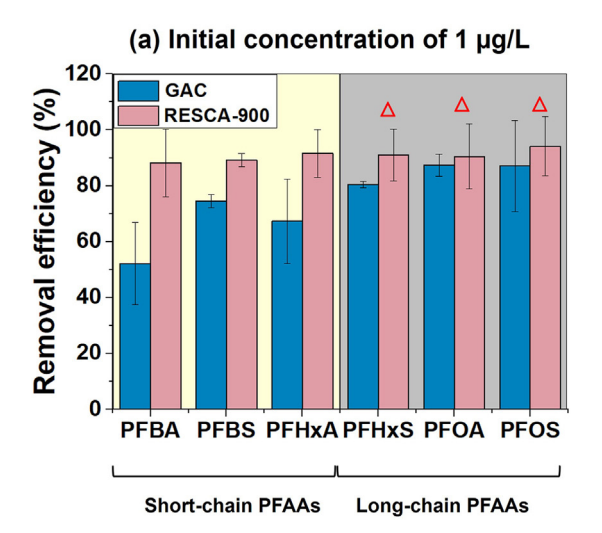
3.1. Effective adsorption of short-chain PFAAs by <u>reed straw-derived biochar (RESCA)</u>

Using PFBA and PFOA as two model compounds representing shortchain and long-chain PFAAs, respectively, the best adsorption efficiencies for both PFAAs were observed for the reed straw-derived biochar (RESCA) synthesized at the highest pyrolysis temperature of 900 °C for 5 h (Fig. 1a to c). We designated this biochar "RESCA-900" for short. PFAA adsorption by biochars was greatly affected by all three manufacturing factors: feedstock material, highest pyrolysis temperature, and pyrolysis duration (Abdul et al., 2017). At an initial concentration of 100  $\mu g/L$ , GAC removed 87  $\pm$  6% of PFOA, but was poor in adsorbing PFBA (13  $\pm$  4%) (Fig. 1a). Anion exchange resin was also effective in removing PFOA (96  $\pm$  2%) and exhibited a slightly better PFBA removal (36  $\pm$  4%) than GAC. Biochars synthesized with carbonrich feedstocks (i.e. corn cobs, reed straws, or aspen chips) showed nearly 100% PFOA removal, implying the important contribution of surface hydrophobicity. Notably, RESCA-900 showed an exceptionally high PFBA removal efficiency of 80  $\pm$  2%. To our knowledge, such effective PFBA adsorption has not been reported by GACs and other carbonbased adsorbents under similar batch conditions (Table S2) (Gagliano et al., 2019; Zhang et al., 2019).

Increase of the highest pyrolysis temperature was key to enhance the PFAA adsorption by RESCAs (Fig. 1b). Adsorption of PFBA was minimal (<5%) by RESCAs pyrolyzed at 500 and 700 °C. Surprisingly, substantial increase in PFBA removal was only observed when the highest pyrolysis temperature was elevated to 900 °C. PFOA adsorption was improved from 60% to 94% when the highest pyrolysis temperature was raised from 500 °C to 700 °C. Complete PFOA removal was achieved when the highest pyrolysis temperature was further elevated to 900 °C. Thus, the highest pyrolysis temperature of 700 °C may be sufficient to generate biochars that are effective for the removal of long-chain PFAAs to the extent comparable to GAC (Fig. 1b), while higher pyrolysis temperature is required for producing biochars for short-chain PFAA removal.

Pyrolysis duration also greatly affected RESCAs' adsorption of PFAAs, particularly PFBA. As shown in Fig. 1c, when the highest pyrolysis temperature was set at 900 °C, a pyrolysis duration of 5 h was optimal. When the pyrolysis duration was shortened to 3 h, little PFBA removal was observed. Pyrolysis for 6 h also negatively affected the adsorption on PFBA. However, adsorption of PFOA was enhanced with the elongation of pyrolysis duration, probably due to the increase of carbon composition and surface hydrophobicity.

Compared to GAC, superior adsorption efficiencies exhibited by RESCA-900 were further evident for six PFAAs of varying chain lengths and moieties at two initial concentrations (1 and 100 µg/L) used in the batch tests (Fig. 2). At an initial concentration of 1 µg/L (Fig. 2a), RESCA-900 removed 92–96% of three short-chain PFAAs (i.e., PFBA, PFBS, and PFHxA), significantly greater than GAC (71–79%). After the adsorption by RESCA-900, concentrations of three long-chain PFAAs



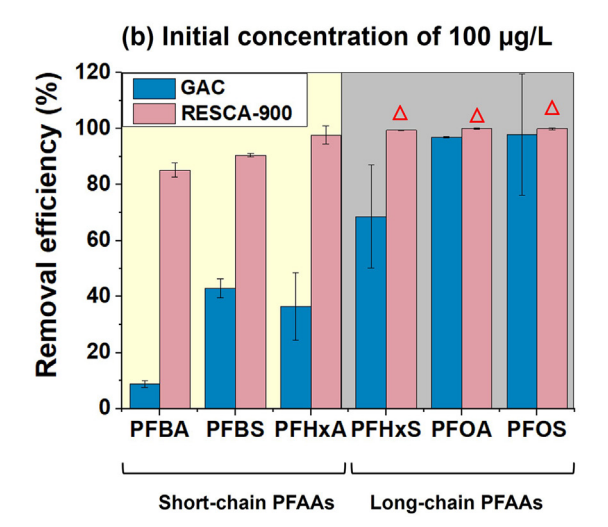


Fig. 2. Removal efficiencies of short-chain and long-chain PFAAs by RESCA-900 and GAC at the initial concentrations of (a) 1 μg/L and (b) 100 μg/L. Red halo triangles on the top of columns represent that concentrations of PFAAs were reduced to below our MDLs (i.e., 30–60 ng/L) after adsorption. The adsorbent dose was 0.2 g/L (For interpretation of the references to colour in this figure legend, the reader is referred to the web version of this article.)

were all below our MDLs (i.e., 30-60 ng/L). This suggests RESCA-900s potential as an adsorbent alternative that can effectively remove PFOS and PFOA at environment-relevant concentrations to meet the stringent EPA health advisory level for both concerned compounds (i.e., 70 ng/L). When the initial concentration increased to  $100 \,\mu\text{g/L}$  (Fig. 2b), removal efficiencies of short-chain PFAAs by RESCA-900 remained high in the range between 80% and 89%. Complete removal of long-chain PFAAs was observed for RESCA-900. However, adsorption by GAC was negatively affected by the increase of PFAA concentration, particularly for the short-chain PFAAs. The rank of PFAA adsorption efficiencies by GAC followed: PFOS (89%) > PFHxS (76%) ≥ PFOA (75%) > PFBS (43%) ≥ PFHxA (38%) > PFBA (18%). This is in good agreement with previous studies on GAC showing better adsorption of PFAAs that are with longer chain length and/or contain the sulfonate group (McCleaf et al., 2017b).

In comparison with previously reported biochar adsorbents (Table S2), RESCA-900 exhibited noticeable improvements in shortchain PFAA adsorption with higher removal efficiencies and/or shorter equilibrium time when an identical or similar initial PFAA concentration and biochar dosage were employed. Most of the previously reported biochars showed poor removal of short-chain PFAAs (mostly <40%) (Dalahmeh et al., 2019; Inyang and Dickenson, 2017; Zhang et al., 2019). Inyang and Dickenson reported 87% PFBA removal by the biochar synthesized with hardwood sawdust pellets via gasification at 900 °C when the initial concentration was 1  $\mu$ g/L. However, the adsorption equilibrium was not achieved until 3 days (Inyang and Dickenson, 2017). In contrast, RESCA-900 can remove 92  $\pm$  1% of PFBA within 24 h (Fig. 2a), revealing its advantages in short-chain PFAA adsorption kinetics and isotherms as detailed below.

### 3.2. Fast kinetics and high capacities for short-chain PFAA adsorption by RESCA-900

Adsorption of both short-chain and long-chain PFAAs was kinetically favorable for RESCA-900 in comparison with GAC (Fig. 3). All kinetic experiments were run for 120 h and adsorption equilibrium was determined when there was no significant change in aqueous concentrations

over at least three sampling points that span for 48 h. At an initial PFAA concentration of 100 µg/L, adsorption equilibrium was achieved by RESCA-900 in 8-12 h and 20-24 h for long-chain and short-chain PFAAs, respectively. Equilibrium was also reached within 24 h for PFAA adsorption by GAC. The pseudo-second-order model was selected to fit the data for the first 24 h of adsorption. Good fitness was revealed by R<sup>2</sup> values that are all greater than 0.82 (Table S3). Pseudo-secondorder kinetic constants (k<sub>2</sub>) for RESCA-900 ranged from 1.137 to 8.38 L/(mg h), which were up to ten times higher than those for GAC (0.10–2.71 L/(mg h)) (Table S3), supporting the rapid PFAA removal exhibited by RESCA-900 (Fig. 3). A recent study by Xiao et al. pointed out a prolonged equilibrium for PFAA adsorption by GAC Calgon F300 due to slow diffusion into internal pores (Xiao et al., 2017). This study also revealed the decrease of particle size can greatly shorten the adsorption equilibrium to less than 24 h. In our study, RESCA-900 and GAC Calgon F820 showed relatively faster adsorption kinetics than GAC Calgon F300 reported in Xiao et al., possibly due to the differences in surface chemistry (detailed in Section 3.3), hydrophobicity, and particle size of the adsorbents, neglecting adsorbate-to-adsorbent ratio and many other experimental factors in batch design from different research studies.

RESCA-900 also showed higher capacities of adsorbing short-chain PFAAs than GAC in our study (Fig. S1 and Table S4). Generally, either Langmuir or Freundlich model fitted well with all isotherm results through nonlinear regression ( $R^2 > 0.8$ ). Based on fitting with the Langmuir isotherm model, the maximum adsorption capacities  $(Q_m)$  for RESCA-900 were 33 to 102% higher for three short-chain PFAAs than those for GAC (Table S4). For two long-chain PFAAs, PFHxS and PFOA, RESCA-900 and GAC exhibited comparable  $Q_m$  values. For PFOS, GAC exhibited greater adsorption capability (55.8 mg/g) than RESCA-900 (34.6 mg/g). Therefore, considering both adsorption kinetics and isotherms, RESCA-900 is more advantageous in removing short-chain PFAAs.

#### 3.3. Hydrophobic surface and uniform mesopores of RESCA-900

Due to the high pyrolysis temperature, RESCA-900 had a highly carbonaceous surface with very few functional groups as revealed by FTIR

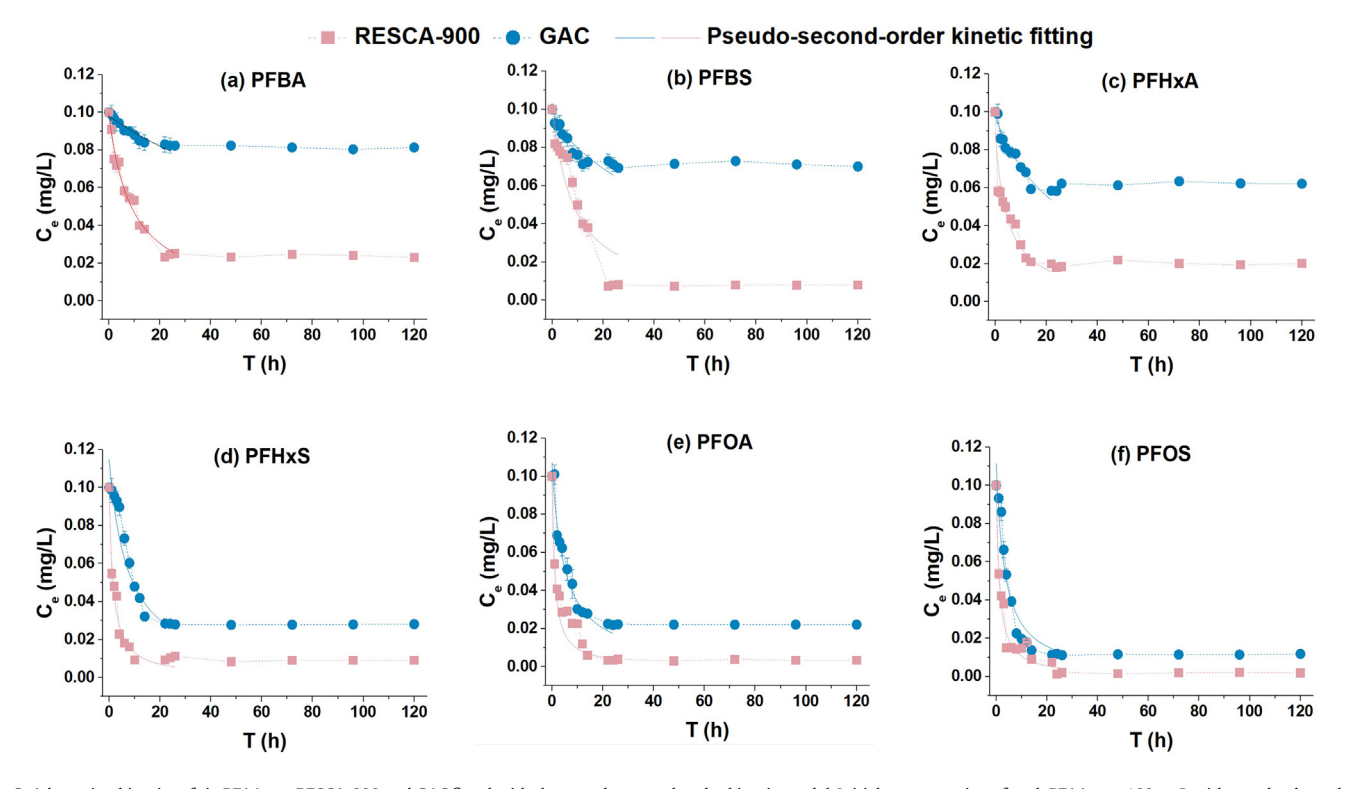


Fig. 3. Adsorption kinetics of six PFAAs on RESCA-900 and GAC fitted with the pseudo-second-order kinetic model. Initial concentration of each PFAA was 100 µg/L with an adsorbent dose of 0.2 g/L. Error bars represent standard deviations among triplicates.

(Fig. S2). Minor vibration stretching for carboxyl and carbonyl groups (2187–2158 cm<sup>-1</sup>) was observed on RESCA-900. Moieties of greater diversities and intensities were found on GAC and the other two RESCAs synthesized at lower pyrolysis temperatures. RESCA-900 also had a relatively large surface area (730 m²/g) driven by the high pyrolysis temperature (Table S5). The combination of large surface area and high carbonation degree was conducive to high surface hydrophobicity of RESCA-900, facilitating its adsorptive interaction with PFAAs, especially the long-chain PFAAs consisting of hydrophobic perfluorinated tails (Deng et al., 2010; Deng et al., 2012).

Uniquely, SEM at  $\times 130,000$  resolution visualized an array of mesopores (2–10 nm in diameter) uniformly distributed on the surface of RESCA-900 (Fig. 4a). Formation of these mesopores on RESCA-900 was also evident by the significant pore volume occupied by pores with diameters in the range between 2 and 6 nm as detected by the BET analysis (Fig. 4b). Minimal mesopores of 2–6 nm in diameter were observed or identified on the surface of GAC or the other two RESCAs synthesized at lower pyrolysis temperatures (Fig. 4b). Existence of these mesopores co-occurred with the significant increase of shortchain PFAA adsorption (Fig. 1b). It is plausible to postulate that these mesopores on the surface of RESCA-900 might facilitate the fast adsorption of short-chain PFAAs considering their small molecular sizes that are typically less than 1 nm in diameter (Table S1). Micropores that

are less than 2 nm in diameter were found abundant among GAC and all RESCAs (Fig. 4b and Table S5). The majority of these micropores are placed inside mesoporous matrixes of these carbonaceous adsorbents, providing additional adsorption sites for PFAAs that diffuse into the particles (Ateia et al., 2018).

To further assess the contribution of electrostatic attraction, PFBA adsorption efficiency and surface charge of RESCA-900 were examined in response to the change of the solution pH. Among the six selected PFAA model compounds, PFBA has the highest pKa value of 0.4 (Table S1), and thus its adsorption is most sensitive to the solution pH. However, as shown in Fig. 4c, there was no significant change in PFBA removal (68-80%) by RESCA-900 when the solution pH was adjusted from 3 to 12. Further, regardless of the pH change, the RESCA-900 surface remained negatively charged as revealed the negative zeta potentials (Fig. 4d). When the pH was between 4 and 11, the zeta potentials of RESCA-900 leveled around -50 mV, reflecting its buffering effect under the aguifer-relevant conditions. Collectively, negligible effects of pH to PFBA adsorption by RESCA-900 and its negative surface charge implied a minor contribution of electrostatic attraction to the observed adsorptive removal of PFAAs. This echoed the lack of moieties (Fig. S2) that are prone to protonation/deprotonation on the surface of this biochar adsorbent (Higgins and Luthy, 2006) (Fig. S2). The AEC of RESCA-900 was below the detection limit, reflecting the minimal presence of

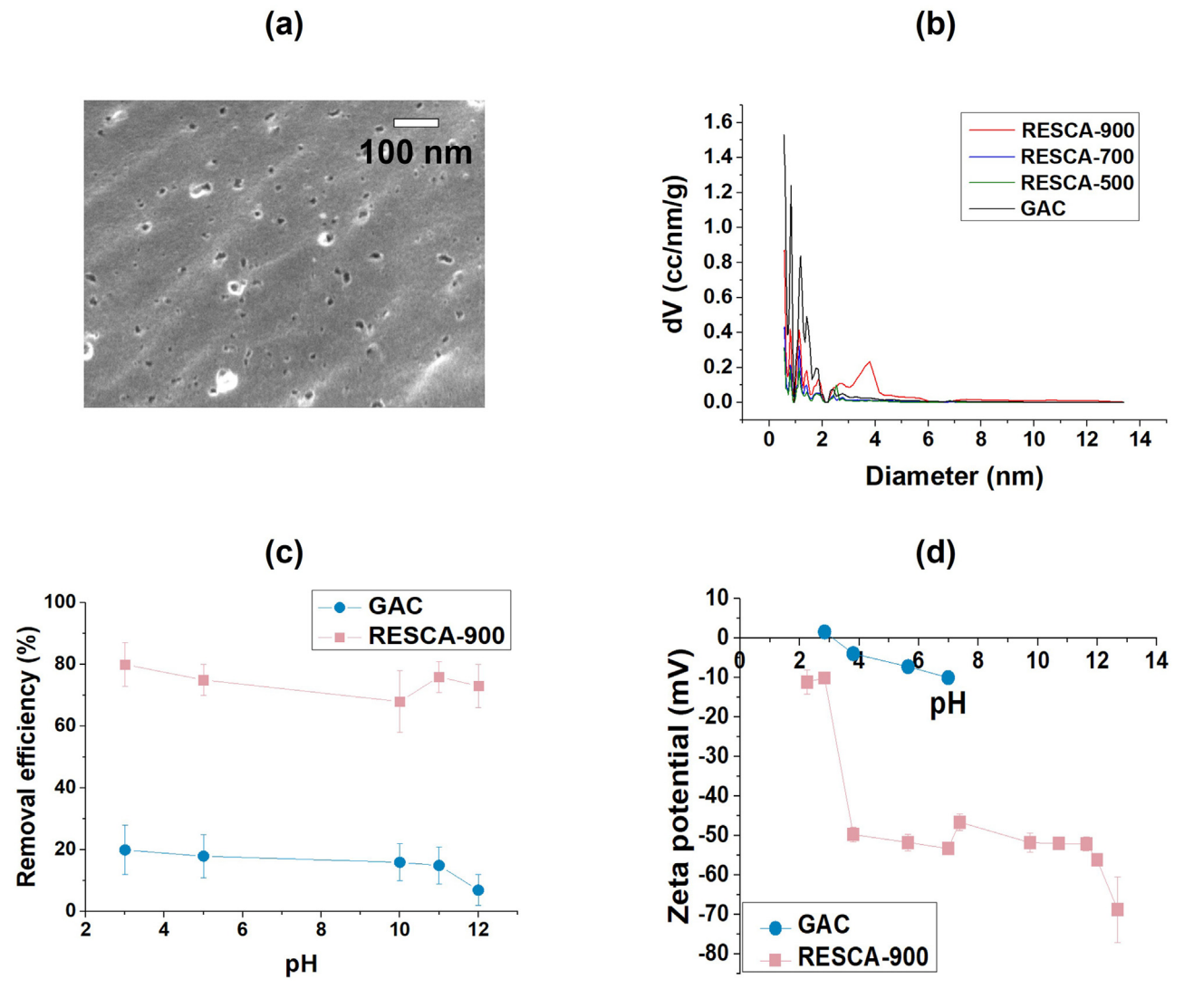


Fig. 4. (a) SEM image showing the mesopores on the surface of RESCA-900 at the magnitude of  $\times$ 130,000; (b) Pore volume distribution for RESCAs and GAC; (c) Effect of pH on PFBA adsorption by RESCA-900 and GAC with an initial PFBA concentration of 100  $\mu$ g/L and an adsorbent dose of 0.2 g/L; (d) Zeta potentials of RESCA-900 and GAC (Loganathan et al., 2018) under different pHs.

positively charged moieties on the surface. Hence, albeit three short-chain PFAAs remain anions in the solution pH above 3, their adsorption by RESECA-900 was dominated by the surface hydrophobicity, rather than electrostatic attraction, considering their surface characteristics (e.g., highly carbonaceous, lack of functional groups or positive charges).

## 3.4. Efficient removal of commingled PFAAs in groundwater by RESCA-900 at high flow rates

In adsorption devices deployed in the field, flow rate is an important operational factor, influencing the contact time for adsorbents with pollutants of concern (e.g., PFAAs). High flow rates are desirable as the dimension of adsorption devices can be reduced, but with the risk of diminishing the removal efficiency caused by the short contact time. Our batch assays revealed RESCA-900s quick adsorption kinetics, eliciting efficient removal of PFAAs of varying chain lengths and functional groups. In order to compare the influence of different flow rates on PFAA removals, 15, 30, 45 mL/min were used in the minifilter tests (Fig. S3) with the constant flow rates controlled by the SPE Vacuum Manifold.

When the flow rate increased from 15 to 30 mL/min, no significant change of PFAA removal efficiencies was observed for filters packed with either RESCA-900 or GAC (Fig. 5). However, further increase of the flow rate to 45 mL/min affected the adsorption performance of filters packed with two adsorbents differently. Surprisingly, RESCA-900-packed filters exhibited significantly higher removal of all PFAAs (>80%) except PFBA (~65%) at the flow rate of 45 mL/min compared to two other slower flow rates. The increase of the flow rate may create external pressure that drives the liquid penetration into internal pores of RESCA-900 packed in the mini-filters. However, for PFBA, which is the most hydrophilic PFAA tested, the promotion on adsorption by the pore penetration was not sufficient to offset the hindrance caused by the shortened contact time, resulting in the decrease in the overall PFBA removal efficiency (Ghaffar et al., 2018; Park et al., 2020).

For GAC filters, an increase of flow rate to 45 mL/min negatively affected the adsorption of short-chain PFAAs, but not long-chain PFAAs. Susceptibility of short-chain PFAAs and resistance of long-chain PFAAs to the increase of the flow rate may be attributed to the slow adsorption kinetics as aforementioned. Pseudo-second-order kinetic factors of GAC for short-chain PFAAs were low in the range of 0.1–0.38 L/(mg h) (Fig. 3 and Table S3). At a flow rate as high as 45 mL/min, the shortened contact time hindered the complete diffusion of PFAA molecules into inner or secondary pores and prohibited dynamic adsorption within multiple interconnected pores in GAC. In contrast, adsorption of short-chain PFAAs in RESCA-900 filters was less kinetically restricted since the adsorption sites are mostly these mesopores that spread on the surface.

Though the mini-filter tests were carried out with six PFAAs, their co-occurrence didn't elicit significant adsorption competition probably

due to adequate amount of adsorbents (RESCA-900 or GAC) packed in the filters. To further examine the competitive adsorption effects, bisolute systems were spiked with PFBA and PFOA as representative compounds for short-chain and long-chain PFAAs, respectively. As shown in Fig. S4, neither the adsorption efficiency nor the equilibrium time was significantly affected for PFBA or PFOA adsorption by the coexistence of both PFAAs in the bisolute system in comparison with the single systems spiked with PFBA or PFOA only. Fast adsorption was also evident for both PFAAs with the equilibrium time of 24 h or shorter regardless of the single or bisolute systems. These results supported the minor influence on PFAA adsorption by the co-existence of other PFAAs at low concentrations (Park et al., 2020). It is noted that these mini-filter tests were all run with pristine adsorbents (RESCA-900 or GAC). Competitive adsorption effects are likely to emerge and exacerbate during the long-term operation in the field as the adsorbents are laden with PFAAs and other chemicals if absorbents are not properly regenerated. This is further discussed in the Supplemental Information about our computation results that profiled PFAA concentration change in the effluents of the full-scale RESCA-900 and GAC columns identical to an actual operating system reported previously (Appleman et al., 2014).

## $3.5. \ Inhibition \ of high \ DOCs \ in \ contaminated \ groundwater \ on \ PFAA \ removal \ by \ RESCA-900$

To further investigate the efficacy of the RESCA-900 filtration for field application, four groundwater samples were collected in triplicate from the center and middle of the plumes at two sites located in California and New Jersey, respectively. As shown in Table S6, two samples CA2 and NJ2 collected within the proximity of the source zones contained relatively high DOCs of 8 and 8.4 mg/L, respectively. The other two samples CA1 and NJ1 were sampled from monitoring wells downstream from the sources and exhibited low DOCs of 1.5 and 2.4 mg/L, respectively. Four samples contained varying diversity and amounts of VOCs and semi-VOCs, such as TCE, 1,1-DCE, benzene, and 1,4-dioxane. It is noted that the detected VOCs and semi-VOCs only accounted for 2-18% of the total DOCs, suggesting the dominance of natural organic matters and other unconcerned chemicals in these groundwater samples. PFAAs were also analyzed using direct injection with LC/ MS/MS, though none of the target PFAAs were detected above the Method Detection Limits (i.e., 30–80 ng/L). Thus, these four samples are good representatives of impacted groundwater for the assessment of remediation efficacies considering their differences in geography, DOC, and co-contaminant composition.

These four groundwater samples were spiked with six PFAAs at an initial concentration of 50  $\mu$ g/L for each PFAA and filtered through mini-filters packed with RESCA-900 or GAC at the flow rate of 30 mL/min. Parallel treatments were prepared with DI water spiked with the same dosage of PFAAs to distinguish the impacts of DOCs and cocontaminants. After filtration through the RESCA-900 or GAC mini-

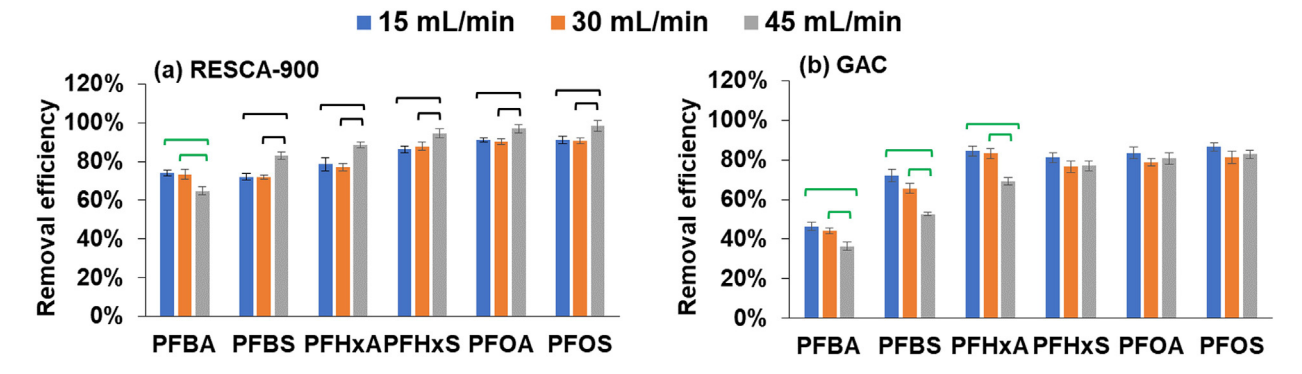


**Fig. 5.** Removal efficiencies of PFAAs after filtration through mini-filters packed with (a) RESCA-900 and (b) GAC at different flow rates. Green and black bars on the top of columns represent PFAA removal efficiencies were negatively and positively affected by the increase of the flow rate, respectively, based on the student *t*-test. (For interpretation of the references to colour in this figure legend, the reader is referred to the web version of this article.)

filters, DOCs in all samples were efficiently removed to below the detection limit of 1 mg/L. In general, RESCA-900 filters exhibited better PFAA removal efficiencies than GAC filters, particularly for the short-chain PFAAs (Fig. S5). Among all four tested samples, the averaged removal efficiencies for RESCA-900 filters were 56% for PFBA, 61% for PFBS, 63% for PFHxA, 73% for PFHxS, 73% for PFOA, and 83% for PFOS. Comparatively, the averaged removal efficiencies for GAC filters were all lower at 27% for PFBA, 39% for PFBS, 56% for PFHxA, 70% for PFHxS, 68% for PFOA, and 76% for PFOS. For long-chain PFAAs, filtration with RESCA-900 and GAC mini-filters achieved effective removals above 65% in most cases. However, for short-chain PFAAs, RESCA-900 filtration removed 50–80%, but filtration with the GAC mini-filters performed poorly with removal efficiencies lower than 50% for PFBA and PFBS, which were in good agreement with the previous observations in this study and others. For instance, removal of PFBA in the groundwater NJ2 (pH: 8.2, TOC: 8.8 mg/L) was as low as 22% by GAC (Fig. S5b). Thus, mere treatment by GAC is inadequate for groundwater heavily impacted by short-chain PFAAs.

To discern the influence of DOC on PFAA adsorption, two-way Mann-Whitney U tests were employed to assess the statistical significance of differences in PFAA removal between samples with high DOCs around 8 mg/L (i.e., CA2 and NJ2) and those with low DOCs around 2 mg/L (i.e., CA1 and NJ1), as well as the controls prepared with DI water. For short-chain PFAAs, significant decrease (p < 0.05) in removal efficiencies by RESCA-900 was observed with the increase of DOC (Fig. 6a, b, and c). Compared to the DI water, short-chain PFAA removal efficiencies by RESCA-900 mini-filters were reduced by 18% (PFBA), 9% (PFBS), 9% (PFHxA) in groundwater samples of low DOCs

and 29% (PFBA), 19% (PFBS), 26% (PFHxA) in groundwater samples of high DOCs on average. Short-chain PFAA adsorption by GAC minifilters was more sensitive to low DOC than RESCA-900, with an average reduction in removal efficiencies of 29% (PFBA), 34% (PFBS), 24% (PFHxA) compared to the DI water controls. However, GAC minifilters also showed tolerance to high DOC as no further significant decrease in removal efficiencies was observed when results from samples of high DOCs and low DOCs were compared.

For both RESCA-900 and GAC mini-filters, negative influence of DOC in groundwater was less profound on long-chain PFAA adsorption compared to short-chain PFAAs. No significant change in PFOS removal efficiencies was observed among all samples regardless of the DOC levels (Fig. 6f). For PFHxS and PFOA, their removal efficiencies were significantly decreased only in groundwater samples with high DOCs, but not in those with low DOCs (Fig. 6d and e). Compared to the DI water controls, groundwater samples with high DOCs exhibited an average removal reduction of 70% in PFHxS and 70% in PFOA for RESCA-900 minifilters and 68% in PFHxS and 62% in PFOA for GAC mini-filters. Overall, RESCA-900 and GAC exhibited similar trends in long-chain PFAA removal in groundwater samples and significant hindrance was only observed at high DOC levels. Adsorption of short-chain PFAAs by RESCA-900 mini-filters gradually decreased in response to the increase of DOCs in the tested groundwater samples. In contrast, inhibition of DOCs to short-chain PFAA removal by GAC mini-filters was more potent even at low DOCs, suggesting GAC is less suited for short-chain PFAA removal in the field. Higher DOC levels in groundwater may result in slower sorption kinetics and lower equilibrium K<sub>d</sub> values (Xing et al., 2008). Thus, when DOC in groundwater is high (e.g., 8 mg/L), it is

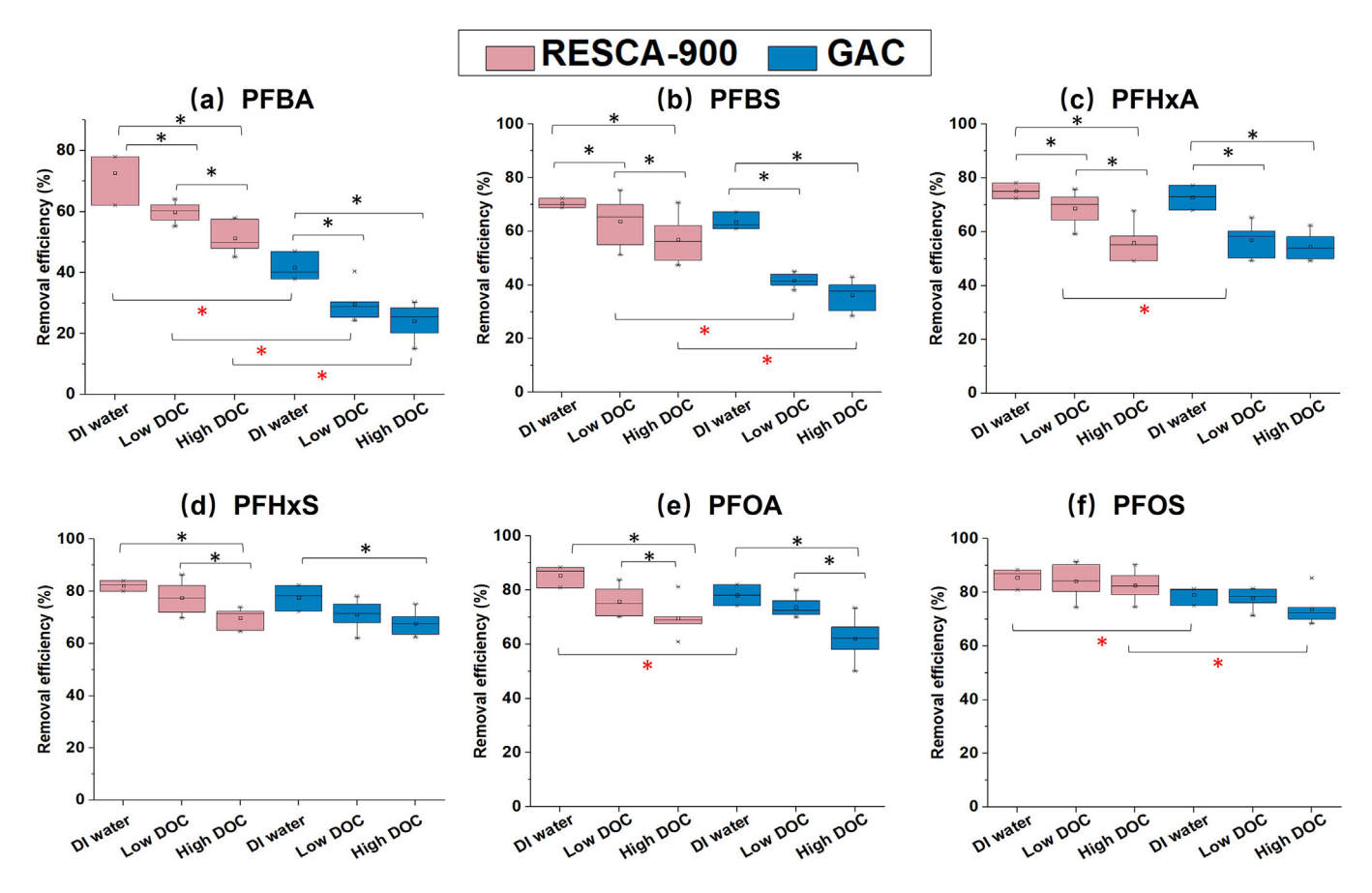


**Fig. 6.** Removal efficiencies of six PFAAs spiked in four groundwater samples with high or low DOCs using RESCA-900 and GAC mini-filters at the flow rate of 30 mL/min. Significant differences between RESCA-900 and GAC filters were tested using two-way Mann-Whitney *U* test (\*, *p* < 0.05). Black asterisks showed significant differences between groundwater and DI-water, while red asterisks showed significant differences between RESCA-900 and GAC filters. (For interpretation of the references to colour in this figure legend, the reader is referred to the web version of this article.)

recommended to implement pre-treatments to reduce DOCs so that the effective adsorption of short-chain PFAAs by RESCA-900 can be enhanced and extended.

#### 4. Conclusions

Overall, a novel green biochar adsorbent RESCA-900 was reported, exhibiting fast and effective adsorption of short-chain PFAAs even at concentrations commonly detected in drinking water and groundwater. While the synthesis of RESCA-900 requires a relatively high pyrolysis temperature, the manufacturing process is sustainable and scalable considering (1) ecological benefits to abate climate change via sequestering carbon from marsh plants that are vigorously growing in temperate regions over the world and (2) possible commercial values to simultaneously produce syn-gas and other fuel chemicals (Woolf et al., 2010). Given GAC's high capacity of adsorbing long-chain PFAAs, sequential carbon adsorption treatment with GAC (primary) and RESCA-900 (secondary) could be an ideal option for remediating comingled contamination of PFAAs, especially when long-chain PFAAs are abundant and/or DOC is high. Primary removal of long-chain PFAAs and other organics by GAC also reduces their competitive inhibition to short-chain PFAA adsorption by RESCA-900 and prolongs its treatment lifespan. Based on PFAA contamination and other geochemical factors in the field, a site-specific treatment train could be designed by leveraging GAC's high adsorption capacities toward long-chain PFAAs and RESCA-900s fast adsorption kinetics toward short-chain PFAAs. Thus, the sequential GAC-RESCA-900 adsorption treatment will ultimately improve the overall PFAA removal efficiency and reduce the operation cost. Such remedial strategy may also be beneficial to mitigate other cocontaminants in the field. In addition, biochar adsorbents are recyclable via regeneration using chemical and thermal treatments. Further modification of their morphology (e.g., size) and surface chemistry can be conducted to tailor their performance and compatibility in different operating systems (e.g., full-scale continuous flow columns). Built on this unique discovery of RESCA-900 adsorbent for PFAA removal, future research is needed to optimize the application values of reed strawderived biochars for water purification and assess their socioeconomical benefits.

#### **CRediT authorship contribution statement**

**Na Liu:** Conceptualization, Methodology, Investigation, Visualization, Validation, Data curation, Writing – original draft. **Chen Wu:** Methodology, Investigation. **Guifen Lyu:** Methodology, Investigation. **Mengyan Li:** Supervision, Conceptualization, Methodology, Writing – review & editing.

#### **Declaration of competing interest**

The authors declare that they have no known competing financial interests or personal relationships that could have appeared to influence the work reported in this paper.

#### Acknowledgments

This work was funded by National Science Foundation, United States (NSF, CBET-1903597), Environmental Protection Agency, United States, New Jersey Water Resources Research Institute (NJWRRI, United States) - Private Well Supplement, and New Jersey Department of Health (NJDOH, United States) - Fostering the Growth of Private Well Researchers at New Jersey's Universities. Na Liu was sponsored by the China Scholarship Council, China (CSC, File No. 201806400016). We appreciate the support of the Faculty Instrument Usage Seed Grant (FIUSG, United States) from the NJIT Otto York Center and technical advice from Dr. Larisa Krishtopa and Dr. Som Mitra for PFAA analysis by LC/MS/MS. We thank Dr. Guangdong Huang for the advice on the simulation work.

We thank Dr. Lucia Rodriguez-Freire and Dr. Wen Zhang for providing the instruments used in this study. We also thank Dr. Joseph Bozzelli (NJIT) for the improvement of the manuscript and Ms. Diana Cutt, Dr. Richard Wilkin, and Dr. Chunming Su (EPA) for their technical advice. Funders had no role in study design, data collection and interpretation, or the decision to submit the work for publication.

#### Appendix A. Supplementary data

Supplementary data to this article can be found online at https://doi.org/10.1016/j.scitotenv.2021.149191.

#### References

- Abdul, G., Zhu, X., Chen, B., 2017. Structural characteristics of biochar-graphene nanosheet composites and their adsorption performance for phthalic acid esters. Chem. Eng. J. 319, 9–20
- Agrafioti, E., Bouras, G., Kalderis, D., Diamadopoulos, E., 2013. Biochar production by sewage sludge pyrolysis. J. Anal. Appl. Pyrolysis 101, 72–78.
- Andersson, E.M., Scott, K., Xu, Y., Li, Y., Olsson, D.S., Fletcher, T., Jakobsson, K., 2019. High exposure to perfluorinated compounds in drinking water and thyroid disease. a cohort study from Ronneby, Sweden. Environ. Res. 108540.
- Appleman, T.D., Higgins, C.P., Quiñones, O., Vanderford, B.J., Kolstad, C., Zeigler-Holady, J.C., Dickenson, E.R., 2014. Treatment of poly-and perfluoroalkyl substances in US full-scale water treatment systems. Water Res. 51, 246–255.
- Ateia, M., Attia, M.F., Maroli, A., Tharayil, N., Alexis, F., Whitehead, D.C., Karanfil, T., 2018. Rapid removal of poly-and perfluorinated alkyl substances by poly (ethylenimine)-functionalized cellulose microcrystals at environmentally relevant conditions. Environ. Sci. Technol. Lett. 5 (12), 764–769.
- Badertscher, M., Bühlmann, P., Pretsch, E., 2009. Structure Determination of Organic Compounds. Springer, Berlin Heidelberg.
- Bischel, H.N., MacManus-Spencer, L.A., Zhang, C., Luthy, R.G., 2011. Strong associations of short-chain perfluoroalkyl acids with serum albumin and investigation of binding mechanisms. Environ. Toxicol. Chem. 30 (11), 2423–2430.
- Blaine, A.C., Rich, C.D., Hundal, L.S., Lau, C., Mills, M.A., Harris, K.M., Higgins, C.P., 2013. Uptake of perfluoroalkyl acids into edible crops via land applied biosolids: field and greenhouse studies. Environ. Sci. Technol. 47 (24), 14062–14069.
- Blanchard, G., Maunaye, M., Martin, G., 1984. Removal of heavy metals from waters by means of natural zeolites. Water Res. 18 (12), 1501–1507.
- Bogdanska, J., Sundström, M., Bergström, U., Borg, D., Abedi-Valugerdi, M., Bergman, Å., DePierre, J., Nobel, S., 2014. Tissue distribution of 35S-labelled perfluorobutanesulfonic acid in adult mice following dietary exposure for 1–5 days. Chemosphere 98, 28–36.
- Brendel, S., Fetter, É., Staude, C., Vierke, L., Biegel-Engler, A., 2018. Short-chain perfluoroalkyl acids: environmental concerns and a regulatory strategy under REACH. Environ. Sci. Eur. 30 (1), 9.
- Buck, R.C., Franklin, J., Berger, U., Conder, J.M., Cousins, I.T., de Voogt, P., Jensen, A.A., Kannan, K., Mabury, S.A., van Leeuwen, S.P., 2011. Perfluoroalkyl and polyfluoroalkyl substances in the environment: terminology, classification, and origins. Integr. Environ. Assess. Manag. 7 (4), 513–541.
- Burkemper, J.L., Aweda, T.A., Rosenberg, A.J., Lunderberg, D.M., Peaslee, G.F., Lapi, S.E., 2017. Radiosynthesis and biological distribution of 18F-labeled perfluorinated alkyl substances. Environ. Sci. Technol. Lett. 4 (6), 211–215.
- Dalahmeh, S.S., Alziq, N., Ahrens, L., 2019. Potential of biochar filters for onsite wastewater treatment: effects of active and inactive biofilms on adsorption of per-and polyfluoroalkyl substances in laboratory column experiments. Environ. Pollut. 247, 155–164.
- Dauchy, X., Boiteux, V., Colin, A., Bach, C., Rosin, C., Munoz, J.-F., 2019. Poly-and perfluoroalkyl substances in runoff water and wastewater sampled at a firefighter training area. Arch. Environ. Contam. Toxicol. 76 (2), 206–215.
- Deng, S., Yu, Q., Huang, J., Yu, G., 2010. Removal of perfluorooctane sulfonate from wastewater by anion exchange resins: effects of resin properties and solution chemistry. Water Res. 44 (18), 5188–5195.
- Deng, S., Zhang, Q., Nie, Y., Wei, H., Wang, B., Huang, J., Yu, G., Xing, B., 2012. Sorption mechanisms of perfluorinated compounds on carbon nanotubes. Environ. Pollut. 168, 138–144.
- Du, Z., Deng, S., Chen, Y., Wang, B., Huang, J., Wang, Y., Yu, G., 2015. Removal of perfluorinated carboxylates from washing wastewater of perfluorooctanesulfonyl fluoride using activated carbons and resins. J. Hazard. Mater. 286, 136–143.
- Felizeter, S., McLachlan, M.S., De Voogt, P., 2012. Uptake of perfluorinated alkyl acids by hydroponically grown lettuce (Lactuca sativa). Environ. Sci. Technol. 46 (21), 11735–11743.
- Gagliano, E., Sgroi, M., Falciglia, P.P., Vagliasindi, F.G.A., Roccaro, P., 2019. Removal of polyand perfluoroalkyl substances (PFAS) from water by adsorption: role of PFAS chain length, effect of organic matter and challenges in adsorbent regeneration. Water Res. 171, 115381.
- Ghaffar, A., Zhu, X., Chen, B., 2018. Biochar composite membrane for high performance pollutant management: fabrication, structural characteristics and synergistic mechanisms. Environ. Pollut. 233, 1013–1023.
- Giesy, J.P., Kannan, K., 2001. Global distribution of perfluorooctane sulfonate in wildlife. Environ. Sci. Technol. 35 (7), 1339–1342.

- Guelfo, J.L., Higgins, C.P., 2013. Subsurface transport potential of perfluoroalkyl acids at aqueous film-forming foam (AFFF)-impacted sites. Environ. Sci. Technol. 47 (9), 4164–4171
- Guo, W., Huo, S., Feng, J., Lu, X., 2017. Adsorption of perfluorooctane sulfonate (PFOS) on corn straw-derived biochar prepared at different pyrolytic temperatures. J. Taiwan Inst. Chem. Eng. 78, 265–271.
- Harris, M.H., Rifas-Shiman, S.L., Calafat, A.M., Ye, X., Mora, A.M., Webster, T.F., Oken, E., Sagiv, S.K., 2017. Predictors of per-and polyfluoroalkyl substance (PFAS) plasma concentrations in 6–10 year old American children. Environ. Sci. Technol. 51 (9), 5193–5204.
- Higgins, C.P., Luthy, R.G., 2006. Sorption of perfluorinated surfactants on sediments. Environ. Sci. Technol. 40 (23), 7251–7256.
- Higgins, C., Field, J., Deeb, R., Conder, J., 2017. FAQs Regarding PFASs Associated with AFFF Use at US Military Sites. Environmental Security Technology Certification Program Alexandria United States
- Inyang, M., Dickenson, E.R., 2017. The use of carbon adsorbents for the removal of perfluoroalkyl acids from potable reuse systems. Chemosphere 184, 168–175.
- Jahnke, A., Barber, J.L., Jones, K.C., Temme, C., 2009. Quantitative trace analysis of polyfluorinated alkyl substances (PFAS) in ambient air samples from Mace head (Ireland): a method intercomparison. Atmos. Environ. 43 (4), 844–850.
- Kim, S.-K., Kannan, K., 2007. Perfluorinated acids in air, rain, snow, surface runoff, and lakes: relative importance of pathways to contamination of urban lakes. Environ. Sci. Technol. 41 (24), 8328–8334.
- Kucharzyk, K.H., Darlington, R., Benotti, M., Deeb, R., Hawley, E., 2017. Novel treatment technologies for PFAS compounds: a critical review. J. Environ. Manag. 204, 757–764.
- Kupryianchyk, D., Hale, S.E., Breedveld, G.D., Cornelissen, G., 2016. Treatment of sites contaminated with perfluorinated compounds using biochar amendment. Chemosphere 142, 35–40.
- Lang, J.R., Allred, B.M., Field, J.A., Levis, J.W., Barlaz, M.A., 2017. National estimate of perand polyfluoroalkyl substance (PFAS) release to US municipal landfill leachate. Environ. Sci. Technol. 51 (4), 2197–2205.
- Lawrinenko, M., Laird, D.A., 2015. Anion exchange capacity of biochar. Green Chem. 17 (9), 4628–4636.
- Lehmann, J., Joseph, S., 2009. Biochar for Environmental Management. Earthscan, London, Sterling, VA.
- Li, F., Duan, J., Tian, S., Ji, H., Zhu, Y., Wei, Z., Zhao, D., 2020. Short-chain per- and polyfluoroalkyl substances in aquatic systems: occurrence, impacts and treatment. Chem. Eng. J. 380, 122506.
- Liu, Y., Li, X., Wang, X., Qiao, X., Hao, S., Lu, J., Duan, X., Dionysiou, D.D., Zheng, B., 2019. Contamination profiles of perfluoroalkyl substances (PFAS) in groundwater in the alluvial plain of Hutuo River, China. Water 11 (11), 2316.
- Loganathan, Paripurnanda, Shim, Wang, Geun, Sounthararajah, Danious, Pratheep, Kalaruban, Mahatheva, 2018. Modelling equilibrium adsorption of single, binary,

- and ternary combinations of Cu, Pb, and Zn onto granular activated carbon. Environ. Sci. Pollut. Res. 25, 16664–16675.
- McCleaf, P., Englund, S., Östlund, A., Lindegren, K., Wiberg, K., Ahrens, L., 2017a. Removal efficiency of multiple poly- and perfluoroalkyl substances (PFASs) in drinking water using granular activated carbon (GAC) and anion exchange (AE) column tests. Water Res. 120, 77–87.
- McCleaf, P., Englund, S., Östlund, A., Lindegren, K., Wiberg, K., Ahrens, L., 2017b. Removal efficiency of multiple poly-and perfluoroalkyl substances (PFASs) in drinking water using granular activated carbon (GAC) and anion exchange (AE) column tests. Water Res. 120, 77–87.
- Nartey, O.D., Zhao, B., 2014. (2014) biochar preparation, characterization, and adsorptive capacity and its effect on bioavailability of contaminants: an overview. Adv. Mater. Sci. Eng. 2014.
- Park, M., Wu, S., Lopez, I.J., Chang, J.Y., Karanfil, T., Snyder, S.A., 2020. Adsorption of perfluoroalkyl substances (PFAS) in groundwater by granular activated carbons: roles of hydrophobicity of PFAS and carbon characteristics. Water Res. 170, 115364.
- Paul, A.G., Jones, K.C., Sweetman, A.J., 2008. A first global production, emission, and environmental inventory for perfluorooctane sulfonate. Environ. Sci. Technol. 43 (2), 386–392.
- Poothong, S., Papadopoulou, E., Padilla-Sánchez, J.A., Thomsen, C., Haug, L.S., 2020. Multiple pathways of human exposure to poly-and perfluoroalkyl substances (PFASs): from external exposure to human blood. Environ. Int. 134, 105244.
- Ross, I., McDonough, J., Miles, J., Storch, P., Thelakkat Kochunarayanan, P., Kalve, E., Hurst, J., Dasgupta, S., Burdick, J., 2018. A review of emerging technologies for remediation of PFASs. Remediat. J. 28 (2), 101–126.
- USEPA, 2016. Drinking Water Health Advisories for PFOA and PFOS.
- Wei, H., Han, L., Tang, Y., Ren, J., Zhao, Z., Jia, L., 2015. Highly flexible heparin-modified chitosan/graphene oxide hybrid hydrogel as a super bilirubin adsorbent with excellent hemocompatibility. J. Mater. Chem. B 3 (8), 1646–1654.
- Woolf, D., Amonette, J.E., Street-Perrott, F.A., Lehmann, J., Joseph, S., 2010. Sustainable biochar to mitigate global climate change. Nat. Commun. 1, 56.
- Xiao, X., Ulrich, B.A., Chen, B., Higgins, C.P., 2017. Sorption of poly-and perfluoroalkyl substances (PFASs) relevant to aqueous film-forming foam (AFFF)-impacted groundwater by biochars and activated carbon. Environ. Sci. Technol. 51 (11), 6342–6351.
- Xing, W., Ngo, H.H., Kim, S.H., Guo, W.S., Hagare, P., 2008. Adsorption and bioadsorption of granular activated carbon (GAC) for dissolved organic carbon (DOC) removal in wastewater. Bioresour. Technol. 99 (18), 8674–8678.
- Zhang, D., He, Q., Wang, M., Zhang, W., Liang, Y., 2019. Sorption of perfluoroalkylated substances (PFASs) onto granular activated carbon and biochar. Environ. Technol. 1–12.